Journal of ELECTRONIC MATERIALS, Vol. 44, No. 6, 2015
DOI: 10.1007/s11664-014-3482-x

Performance of Novel Thermoelectric Cooling Module Depending on Geometrical Factors

NAIM DEREBASI,[1,4] MUHAMMED ELTEZ,[2] FIKRET GULDIKEN,[1] AZIZ SEVER,[2] KLAUS KALLIS,[3] HALIL KILIC,[2] and EMIN N. OZMUTLU[1]

1.—Department of Physics, Uludag University, Gorukle Bursa, Turkey. 2.—GK Projects GmbH, Duisburg, Germany. 3.—TU-Dortmund, Dortmund, Germany. 4.—e-mail: naim@uludag.edu.tr

A geometrical shape factor was investigated for optimum thermoelectric performance of a thermoelectric module using finite element analysis. The cooling power, electrical energy consumption, and coefficient of performance were analyzed using simulation with different current values passing through the thermoelectric elements for varying temperature differences between the two sides. A dramatic increase in cooling power density was obtained, since it was inversely proportional to the length of the thermoelectric legs. An artificial neural network model for each thermoelectric property was also developed using input–output relations. The models including the shape factor showed good predictive capability and agreement with simulation results. The correlation of the models was found to be 99%, and the overall prediction error was in the range of 1.5% and 1.0%, which is within acceptable limits. A thermoelectric module was produced based on the numerical results and was shown to be a promising device for use in cooling systems.

Key words: Thermoelectric cooling module, cooling performance, finite element method, artificial neural network

INTRODUCTION

Recently, thermoelectric cooler (TEC) modules have been applied for electronic cooling. TEC modules are widely used in military, aerospace, instrument, and industrial products for different cooling purposes, offering the advantages of small size, quiet operation, and reliability.[1]

Thermoelectric refrigeration is achieved when a direct current is passed through one or more pairs of *n*- and *p*-type semiconductor materials. In the cooling mode, direct current passes from the *n*- to *p*-type semiconductor material. The refrigeration capability of a semiconductor material is dependent on the combined effect of the material's Seebeck voltage, electrical resistivity, and thermal conductivity over the operating temperature range between the cold and hot ends.[2–4]

(Received July 15, 2014; accepted October 15, 2014; published online November 5, 2014)

The coefficient of performance (COP) for thermoelectric technology is lower than that for conventional cooling systems. Therefore, much research has focused on improvement of the COP of thermoelectric cooling systems by means of developing new materials for use in TEC modules, optimization of the module systems design, fabrication methods, and improvement of the heat exchange efficiency.[5–12] However, little research has investigated the performance of cooling modules, including the geometrical dimensions of the *p*- and *n*-type semiconductor thermoelectric elements of TEC modules.[6]

This research focused on optimization of the thermal properties of a TEC module including geometrical factors of the *p*- and *n*-type semiconductor pellets. Therefore, the thermoelectric cooling power, electrical energy consumption, and COP were obtained by numerical methods, namely simulation by a finite element method (FEM) and prediction by artificial neural network (ANN), to determine the optimum dimensions of the TEC module.

THEORY OF THERMOELECTRIC COOLING

A typical TEC module consists of p- and n-type pellets connected electrically in series and sandwiched between two ceramic substrates (Fig. 1). When a direct current passes through such a circuit of heterogeneous thermoelectric conductors, it causes a temperature difference between the two sides of the TEC module. As a result, one TEC face (called the cold side) will be cooled while its opposite face (called the hot side) will be simultaneously heated. This phenomenon is known as the Peltier effect.[13,14] The thermoelectric heat (Q) pumped by the Peltier effect at the cold end of a thermoelectric couple as shown in Fig. 2 is given by

$$Q = \alpha I T_c, \tag{1}$$

where α, I, and T_c are the Seebeck coefficient, the direct current passing through the thermoelectric material, and the cold-side temperature in Kelvin, respectively. Current flow generates Joule heat (Q_J) in the thermoelectric material, which goes equally to the cold and hot ends:

$$Q_J = I^2 R, \tag{2}$$

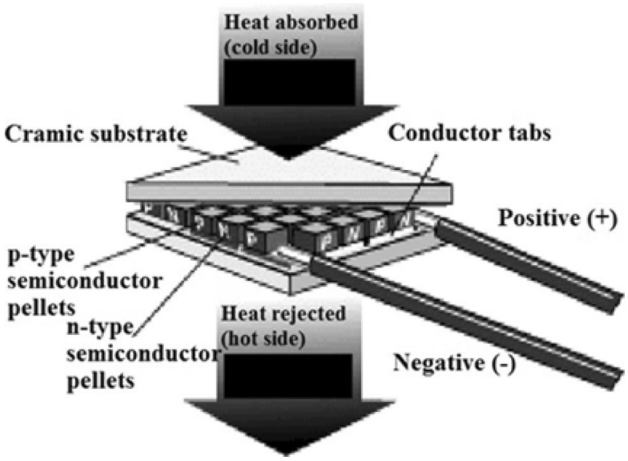

Fig. 1. Typical TEC module.[14]

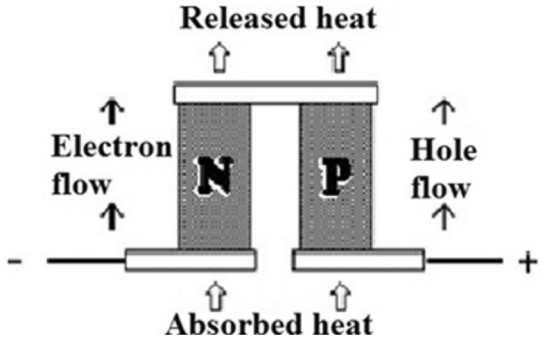

Fig. 2. Thermoelectric heat pumping by the Peltier effect in a thermoelectric couple.[14]

where R is the resistance of the thermoelectric material, defined as

$$R = \frac{\rho}{G}, \tag{3}$$

where ρ is the resistivity and G is the geometrical shape factor of the thermoelectric pellet:

$$G = \frac{A}{L}, \tag{4}$$

where A is the cross-sectional area and L is the length of the thermoelectric element. During operation, heat is conducted by electrons from the hot to the cold end through the thermoelectric material. The rate of heat conduction (Q_{hc}) is given by

$$Q_{hc} = k(T_h - T_c) = k\Delta T, \tag{5}$$

where k and ΔT are the thermal conductance and temperature difference between the hot and cold sides of the thermoelectric couple, and k can be defined as

$$k = \lambda G, \tag{6}$$

where λ is the thermal conductivity of the thermoelectric material. Combining Eqs. 1, 2, and 5 and substituting Eqs. 4 and 6 into an energy balance at the end of the thermoelectric couple gives

$$Q_c = \alpha I T_c - \frac{I^2 \rho}{2G} - \lambda G \Delta T. \tag{7}$$

The electrical energy consumption (Q_P) of the couple is given by

$$Q_P = \frac{I^2 \rho}{G} + \alpha I \Delta T. \tag{8}$$

The electrical power consumption of a thermoelectric couple is used to generate Joule heat and overcome the Seebeck effect, which generates power due to the temperature difference between the two junctions of the couple. The COP of a thermoelectric couple for cooling is given by

$$\mathrm{COP} = \frac{Q_c}{Q_P} = \frac{\alpha I T_c - \frac{I^2\rho}{2G} - \lambda G \Delta T}{\frac{I^2\rho}{G} + \alpha I \Delta T}. \tag{9}$$

The COP of a thermoelectric material is a combined effect of its Seebeck coefficient, electrical resistivity, geometrical dimensions, and thermal conductivity over the operating temperature range between the cold and hot ends. The performance of a thermoelectric material is called the figure of merit (Z) and is expressed as

$$Z = \frac{\alpha^2}{\lambda \rho} = \frac{\alpha^2}{\lambda R G}. \tag{10}$$

Each of the n- and p-type thermoelectric material properties varies as a function of temperature, so the figure of merit for each material is also temperature

dependent. Maximizing the figure of merit is an important objective during the selection and optimization of thermoelectric materials as it limits the temperature difference, whereas the G factors for the n- and p-type materials define the heat pumping capacity. The most widely used thermoelectric material for cooling in the temperature range of 0°C to 200°C is bismuth telluride (Bi_2Te_3), due to its advantageous thermal properties compared with other thermoelectric materials such as PbTe and SiGe (Fig. 3).[15]

SIMULATION AND PREDICTIONS

Simulation by FEM

A TEC module must have optimum thermal properties and geometrical dimensions to achieve the best performance. Therefore, to improve the COP for cooling, one must take into account variables including the optimum current, temperature difference, thermoelectric material, electrical resistivity, and thermal conductivity. The optimum current is calculated theoretically from $\frac{\partial \mathrm{COP}}{\partial I} = 0$. The temperature difference $\left[\Delta T = \frac{1}{2}(T_h + T_c)\right]$ depends on the hot- and cold-end temperatures. The best thermoelectric material for cooling in the range of 0°C to 200°C is Bi_2Te_3 due to its Seebeck coefficient. The electrical resistivity and thermal conductivity of Bi_2Te_3 show better characteristics compared with other thermoelectric materials in this temperature range.[15] However, the geometrical shape factor G must be investigated for different dimensions.[16]

Thin-film thermoelectric coolers have potential advantages. The main benefit of using a thin-film cooler is the dramatic increase in the cooling power density, since it is inversely proportional to the length of the thermoelectric legs.[17] As shown in Fig. 4, achievement of a cooling power density above 100 W/cm^2 is possible for cooler leg lengths on the order of 20 μm to 50 μm.

Four different TEC modules with 15 identical pairs of p- and n-type square semiconductor pellets were modeled (Fig. 5a).[18] The semiconductor p- and n-type pellets were made of Bi_2Te_3 material with varied leg length (L) and width (w), being connected electrically in series and thermally in parallel to each other using silver metal plates; the square sandwich material with area S was chosen as Al_2O_3 ceramic. The geometrical dimensions of the pellets for the TEC modules are presented in Table I.

Thermoelectric cooling simulations were carried out using ANSYS® Workbench modeling software. The thermal and electrical scalar potential vectors were calculated using the FEM.[19] The element types used for FEM analysis were hexagonal and tetragonal, after carrying out many iterations to obtain the optimum mesh for solving the problem (Fig. 5b). A homogeneous mesh was preferred, since there were no critical areas that would affect the results. The hexagonal mesh was used for the n- and p-type semiconductor pellets, while a free tetragonal mesh was used for the silver conductors and ceramic plates. The hot-side temperature was kept constant at 330 K, while the cold-side temperature was varied in the range from 260 K to 325 K. The cooling power (Q_C), electrical energy consumption (Q_P), and COP were simulated for different current values passing through the thermoelectric elements for various temperature differences between the two sides.

Figure 6 shows thermal analysis of the TEC modules obtained from models 1, 2, 3, and 4. In model 1 (Fig. 6a), the cooling power increases with the current passing through the pellets up to about 80 A, then slightly decreases at higher current values above 80 A. The maximum Q_C value is achieved when the cold-side temperature is 325 K. In models 2 and 3, Q_C shows the same trend with increasing current as in model 1. However, the current reduces when the shape factor G is decreased. The results for model 4 are very significant. The current passing thorough the thermoelectric pellets is reduced 10^4-fold, while the cooling power is increased 10^4-fold (Fig. 6d). Also, the length of the thermoelectric legs is reduced from

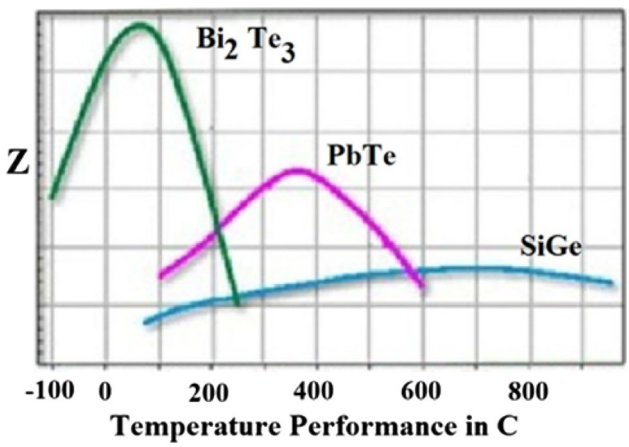

Fig. 3. Variation of figure of merit with temperature for different thermoelectric materials.[15]

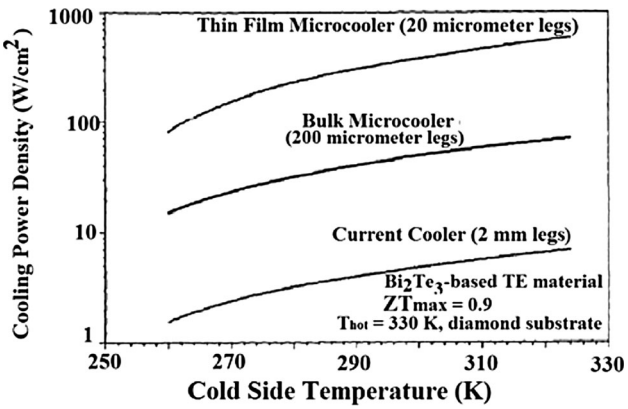

Fig. 4. Variation of cooling power density with cold-side temperature for different G factors.[16]

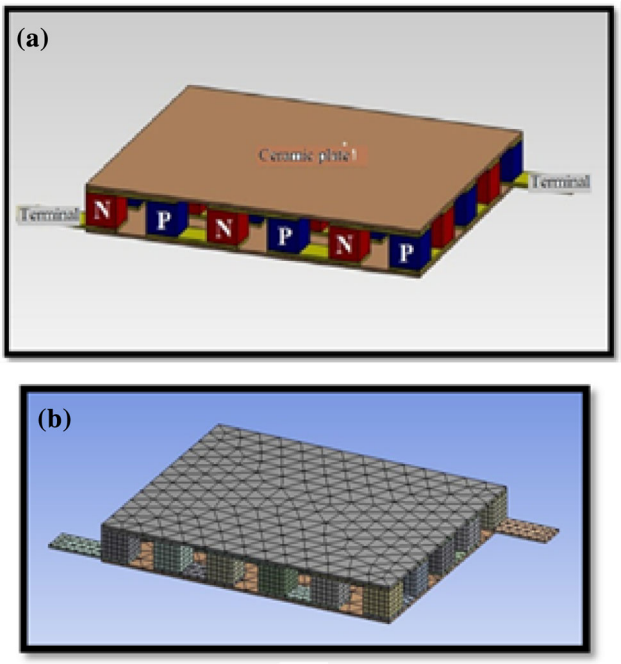

Fig. 5. (a) Modeling and (b) meshing of a TEC module.

Table I. Geometrical dimensions of the modeled TEC modules

Module No.	*L*	*w*	*S*
1	1 cm	1 cm	100 cm^2
2	1 mm	1 mm	100 mm^2
3	100 μm	100 μm	1 mm^2
4	1 μm	1 μm	100 μm^2

1 cm to 1 μm, i.e., a 10^4-fold reduction. Therefore, these results are in good agreement with the theory stating that thin-film coolers will exhibit a dramatic increase in cooling power density, since it is inversely proportional to the length of the thermoelectric legs (Fig. 7). The thermoelectric cooling was directly related to the effective area for cooling. The cooling performance in model 4 at 325 K reached about 1.4 kW, whereas it was only 1.4 W in model 1 for the same temperature gradient.

ANN Predictions

Use of artificial neural networks has become popular during the last decade.[20,21] The reason for this is that neural networks represent a novel and modern approach that can provide solutions to problems for which conventional mathematics, algorithms, and methodologies are unable to find a satisfactory and acceptable solution. ANNs are inspired by the functionality and structure of the human brain, which can be imagined as a network comprising densely interconnected elements called neurons.[22]

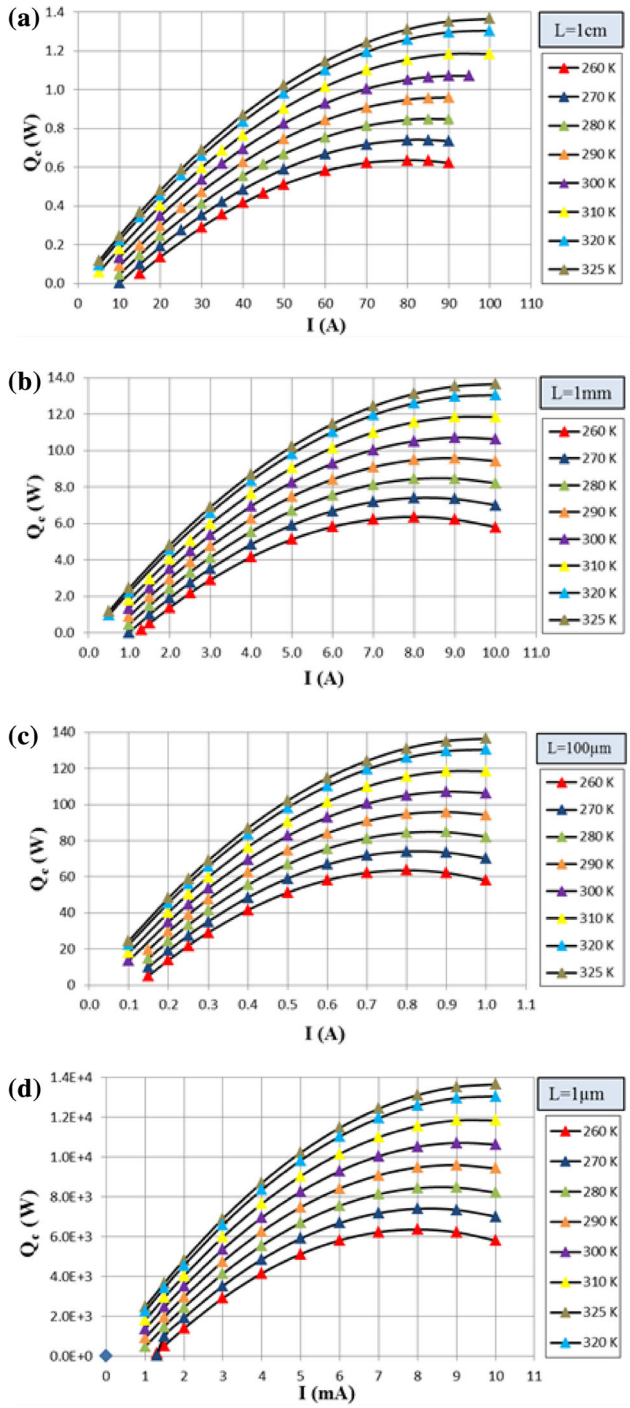

Fig. 6. Variation of cooling power with current passing through the pellets for TEC models (a) 1, (b) 2, (c) 3, and (d) 4 for the temperature range of 260 K to 325 K.

The most popular neural network is the multilayer perceptron, which is a feed-forward network; i.e., all signals flow in a single direction from the input to the output of the network. It consists of neurons organized in a number of layers that can be categorized into three parts: the first part is the input layer, which allows the network to communicate with the environment; the second part is

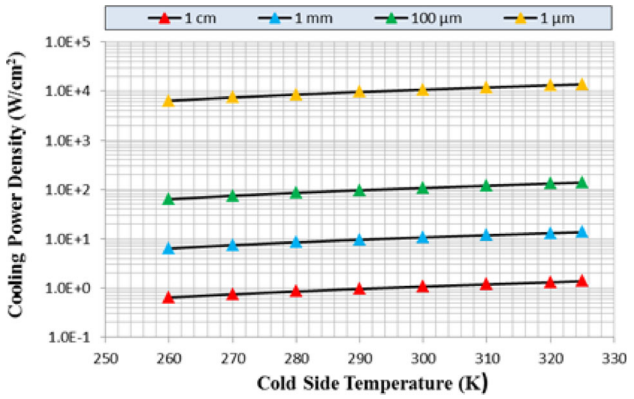

Fig. 7. Variation of cooling power density with cold-side temperature for unit area.

commonly known as the hidden part, in which one or more layers of neurons exist depending on the problem's demands and requirements for generalization; and the third part is the output layer.[23]

The artificial neurons are arranged in layers, wherein the input layer receives inputs from the real world and each successive layer receives weighted outputs from the preceding one as its input, thereby resulting in a feed-forward ANN where each input is fed forward to the subsequent layer for treatment. The outputs of the last layer constitute the outputs to the real world.

Training data from FEM analysis of a sample of four TEC modules were obtained for dimensions with length and width ranging from 1 cm to 1 μm and ceramic plate area from 100 cm^2 to 100 μm^2. In the proposed neural network models, the input parameters were the cold-side temperature (T_c), the length (L), width (w), and area (S) of the thermoelectric leg, the current passing through them (I), and the voltage across the terminals of the TEC module (V), while the output parameters were the cooling power (Q_C), electrical energy consumption (Q_P), and COP.

Qnet 2000®,[24] a commercial neural network package, was used for the first time in the prediction of the performance of a TEC module, offering the advantage of rapid network development through flexible choices of algorithms, output functions, and other training parameters, thereby enhancing accuracy. A total of 357 input vectors obtained from the four TEC modules modeled by FEM analysis for Q_C, Q_P, and the COP were available in the training set for a back-propagation neural network. The number of hidden layers and neurons in each layer were determined by trial and error to be optimal, including different transfer functions such as hyperbolic tangent, sigmoid, and hybrid. After the network had been trained, better results were obtained from the network formed by the hyperbolic tangent transfer function in the hidden layers and the sigmoid transfer function in all output layers for prediction of Q_C, Q_P, and the COP. These transfer functions are

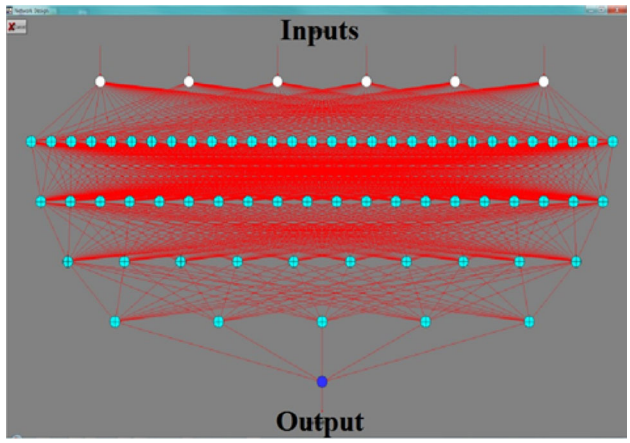

Fig. 8. ANN developed for the COP.

Table II. Contribution of input nodes to estimated thermoelectric properties of TEC modules in ANN models

Input Node	Contribution (%)		
	Q_C	Q_P	COP
T_c	6.28	1.19	22.70
L	5.40	3.60	1.22
w	2.80	3.50	1.16
S	8.86	1.01	0.70
I	65.79	85.07	3.10
V	10.87	5.64	71.13

$$\tanh x = \frac{e^{x} - e^{-x}}{e^{x} + e^{-x}}, \tag{14}$$

$$\text{sigmoid} = \frac{1}{1 + e^{-x}}. \tag{15}$$

The networks included 6 input neurons, 1 output neuron, and four hidden layers with 65 neurons for Q_P and the COP and 75 neurons for Q_C, with full connectivity between nodes (Fig. 8). Back-propagation ANNs require that all training input data must be normalized to improve the training characteristics. Therefore, all data for the nodes in the input layer and training targets for the output layer were normalized between the limits of 0.15 and 0.85.

The performance of the ANN model was measured statistically based on the root-mean-square error and average correlation. A set of test data for Q_C, Q_P, and the COP, different from the training data, was used to investigate the network performance. The average correlation and maximum prediction error were found to be 99% and 1.5%, respectively, for the TEC modules tested. Table II also presents the percentage contribution of the input nodes. All tested modules in the range of

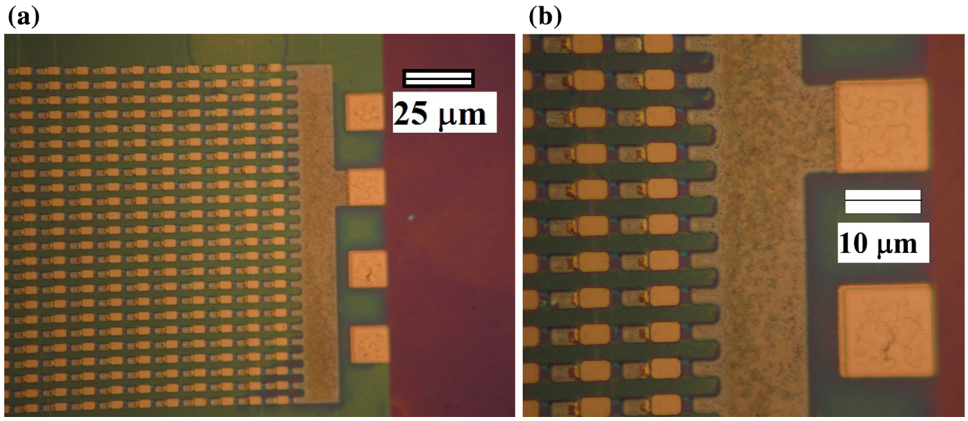

Fig. 9. Different views of samples prepared by the lithography technique: (a) edge of module and (b) magnified image.

the training data showed very high correlation coefficients. The ANN model was assessed using a TEC module with dimensions of $L = w = 1$ mm and $S = 100$ mm^2 at $T_c = 290$ K, which lies outside the range of the training data.

From Table II, it is clear that the width of the thermoelectric leg w makes a minimum contribution, while the current passing through the pellets makes the major contribution to the prediction of Q_C. The cross-sectional area S also makes a minimum contribution to either Q_P or the COP, while the current passing through the pellets makes a maximum contribution to Q_P and the voltage across the terminals of the TEC module makes a major contribution to the prediction of the COP. The developed ANN models have acceptable prediction capability for the thermoelectric properties of the TEC modules within the defined training dataset and good correlation with acceptable accuracy between the simulated and predicted results.

Experimental Procedures

Fabrication of the prototype started with a double-side-polished 670-μm-thick Al_2O_3 wafer. Then, p- and n-type semiconductor thermoelectric elements were obtained using Bi_2Te_3 doped with 1% selenium and 1% antimony, respectively. TiN composite was used as an adhesion layer while the material titanium Ti as a bottom layer connector was developed in spite of Ag/Au and the top connector layer was formed from the aluminum material. Between Al_2O_3 and Bi_2Te_3 there is always a TiN adhesive layer of 95 nm height, which is never directly connected to the bottom connector (Ti).

The Plasma 80 sputtering technique was used for the samples, which were annealed for 30 min at 1350°C for prebaking. A hexamethyldisilane (HMDS) gas flow was also used. The spinner speed was 3500 rpm for 30 s, followed by annealing for 60 s at 1000°C for baking. The MA4 lithography technique (EUV) was used for 18 s. The prototypes were also annealed for 30 min at 1350°C for hard-baking. The developer used was an AZ device using 2:1 diluted water. The reactive ion etching method was utilized to etch the sample with a resist etching time of 10 min at 1350°C with drying after the cleaning process. Ellipsometry and scanning electron microscopy (SEM) techniques were used to observe the samples. Figure 9 shows the samples obtained using this procedure.

CONCLUSIONS

The geometrical shape factor G was investigated for optimum thermoelectric properties of a TEC module. The cooling power Q_C, electrical energy consumption Q_P, and COP were analyzed using simulations with different current values passing through the thermoelectric elements for various temperature differences between the two sides. The variation of the cooling power Q_C, the low electrical energy consumption Q_P, and the high COP value indicate that a significant contribution can be made to cooling challenges and technology. One of the significant contributions of the simulation results could be a solution to cooling challenges in the field of semiconductor applications and technology. The COP is inversely proportional to the length of the thermoelectric legs and can be increased every 4 years. The ANN models developed including the G shape factor showed good predictive capability with acceptable accuracy compared with simulation results. The results of all the developed ANN models were in good agreement with simulation results. The average correlation of the models was found to be 99%, and the overall prediction error was in the range of 1.5% and 1.0%, which is within the acceptable limits for thermoelectric properties. These models could be useful tools for designers to assess thermoelectric module performance before production of a TEC module, saving time and material use.

ACKNOWLEDGEMENTS

This research is part of the physics Ph.D. thesis of Naim Derebasi and is under the protection of PCT

patent no. PCT/EP2013/2081094. The authors would like to thank GK Projects GmbH for allowing publishing of the presented research, ALDO B&W Energy Co. for financial support, and Ms Filiz Sagliker ELSA Co. for personnel assistance.

REFERENCES

1. Y.W. Chang, C.H. Cheng, W.F. Wu, and S.L. Chen, *Int. J. Eng. Appl. Sci.* 4, 173 (2008).
2. S.B. Riffat and X. Ma, *Appl. Therm. Eng.* 23, 913 (2003).
3. T.M. Tritt and M.A. Subramanian, *MRS Bull.* 31, 188 (2006).
4. S.B. Riffat and X. Ma, *Int. J. Energy Res.* 28, 753 (2004).
5. J.P. Fleurial, G.J. Snyder, J.A. Herman, M. Smart, and P. Shakkottai, *34th Int. Soc. Energy Conversat. Eng. Conf. Proc.* Vancouver, BC, Canada, 992569 (1999).
6. P. Arunkumar, P. Iswarya, S. Supraja, P. Rajarayan, and G. Balaj, *Int. J. Comput. Commun. Inf. Syst.* 2, 28 (2010).
7. S.B. Riffat, X. Ma, and R. Wilson, *Appl. Therm. Eng.* 26, 494 (2006).
8. L. Chen, F. Meng, and F. Sun, *Rev. Mex. Fis.* 55, 282 (2009).
9. S.B. Riffat and X. Ma, *Int. J. Energy Res.* 28, 1231 (2004).
10. H.J. Goldsmid, *J. Thermoelectr.* 4, 14 (2005).
11. K. Atik, *5th Int. Adv. Technol. Symp* (Turkey: Karabük University, 2009).
12. N. Wang, C.H. Wang, J.X. Lei, and D.S. Zhu, *Int. Conf. Electron. Pack. Technol. & High Density Pack.*, IEEE (2009).
13. A.F. Ioffe, *Infosearch*, London (1957).
14. D.M. Rowe, *Thermoelectrics Handbook Macro to Nano* (Boca Raton: CRC Taylor & Francis, 2006).
15. A. Bar-Cohen, G.L. Solbrekken, and K. Yazawa, *IEEE Trans. Adv. Packag.* 28, 2 (2005).
16. R.E. Simons and R.C. Chu, *16th IEEE Semi-Therm. Symp.* (2000).
17. J.W. Vandersande and J.P. Fleurial, *Proc. 15th Int. Conf. Thermoelectrics*, 37 (1997).
18. F. Guldiken, *M.Sc. Thesis*, Uludag University, Bursa Turkey (2011).
19. P.P. Silvester and R.L. Ferrari, *Finite Elements for Electrical Engineers*, 3rd ed. (Cambridge: Cambridge University Press, 1996).
20. G.K. Miti, A.J. Moses, N. Derebasi, and D. Fox, *J. Magn. Magn. Mater.* 254, 262 (2003).
21. M. Laidi and S. Hanini, *Int. J. Refrig.* 36, 247 (2013).
22. K. Gurney, *An Introduction to Neural Networks* (London: UCL Press, 1999).
23. D. Graupe, *Principles of Artificial Neural Networks* (Singapore: World Scientific, 1997).
24. Qnet2000 Help Manual.